Ultrafast Photochemistry in Liquids

Arnulf Rosspeintner, Bernhard Lang, and Eric Vauthey

Department of Physical Chemistry, University of Geneva, CH-1211 Geneve 8, Switzerland; email: Eric.vauthey@unige.ch

Annu. Rev. Phys. Chem. 2013. 64:247–71

First published online as a Review in Advance on January 4, 2013

The *Annual Review of Physical Chemistry* is online at physchem.annualreviews.org

This article's doi: 10.1146/annurev-physchem-040412-110146

Keywords

vibrational relaxation, solvation dynamics, electron transfer, proton transfer, photoisomerization

Abstract

Ultrafast photochemical processes can occur in parallel with the relaxation of the optically populated excited state toward equilibrium. The latter involves both intra- and intermolecular modes, namely vibrational and solvent coordinates, and takes place on timescales ranging from a few tens of femtoseconds to up to hundreds of picoseconds, depending on the system. As a consequence, the reaction dynamics can substantially differ from those usually measured with slower photoinduced processes occurring from equilibrated excited states. For example, the decay of the excited-state population may become strongly nonexponential and depend on the excitation wavelength, contrary to the Kasha and Vavilov rules. In this article, we first give a brief account of our current understanding of vibrational and solvent relaxation processes. We then present an overview of important classes of ultrafast photochemical reactions, namely electron and proton transfer as well as isomerization, and illustrate with several examples how nonequilibrium effects can affect their dynamics.

1. INTRODUCTION

Donor-acceptor (DA) complex: intermolecular complex between two molecules with opposite redox properties and characterized by a UV-visible absorption band due to a charge-transfer transition between the two constituents

Since the first direct experimental observations of molecular dynamics in the gas and condensed phases (1–3), ultrafast spectroscopy has emerged into a multidisciplinary and active domain of research. In this review, we present a selection of recent works that give a representative overview of the activities in the field of ultrafast photochemical reactions in the liquid phase.

During the first few picoseconds after excitation, photochemical and photophysical processes are accompanied by various relaxation processes of the nuclear degrees of freedom. In many cases, these relaxation processes are much faster than the studied reaction itself, which leads to the well-known rules stated by Kasha and Vavilov (4). The situation is very different with ultrafast photochemical reactions, in which the reactants start to propagate along the reaction coordinate before the nuclear coordinates have relaxed to the equilibrium configuration of the excited state. **Figure 1** illustrates the processes and timescales typically involved in ultrafast photoinduced reactions. Barrierless proton transfer (PT) and electron transfer (ET) may occur on times as short as a few tens of femtoseconds (5–8). Isomerization processes that do not involve large-amplitude motions and bimolecular ET in strongly coupled donor-acceptor (DA) pairs can take place in less than 1 ps (9–13). Comparatively, dynamical processes related to the solvent, such as solvation dynamics, cooling, and diffusional transport, may take much longer, depending on solvent properties such as viscosity (14–17). As there is no separation between the timescales of relaxation and reaction, the relaxation processes may influence or even control the outcome of the chemical reaction.

Conservation of momentum and kinetic energy during photoexcitation leads to the Franck-Condon principle, which states that the configuration of the nuclei is practically frozen during the interaction with the optical field. The solute is thus brought to an electronically excited state, whereas the nuclear degrees of freedom of both the solute and solvent are still in the equilibrium configuration of the solute's electronic ground state. Hence the internal and external nuclear degrees of freedom are out of equilibrium with respect to the excited-state electronic configuration.

At this early stage within the first hundred femtoseconds after photoexcitation, the chromophore and its first solvation shell undergo the so-called inertial response. The coherent superposition of vibrational levels created during excitation often leads to coherent wave-packet

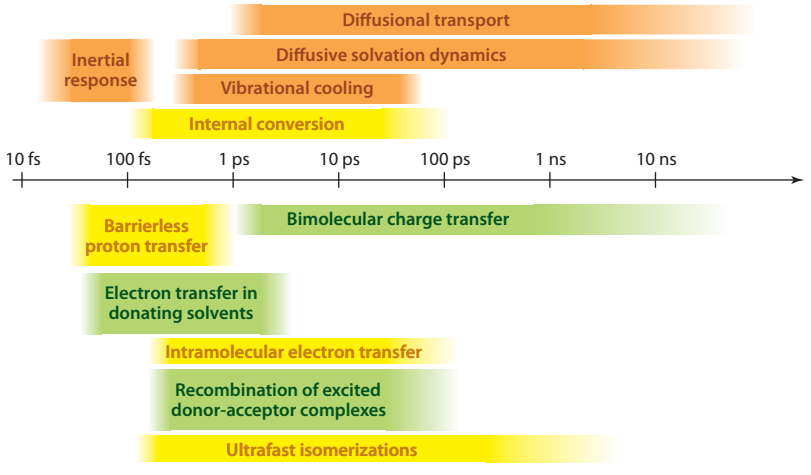

Figure 1

Timescales of the ultrafast photophysical and photochemical processes discussed in this article.

dynamics in the excited-state potential manifold, which is of quasi-reversible character (18–20). The coupling to fluctuating intra- and intermolecular modes leads to subsequent dephasing and transforms the initial coherent dynamics into kinetics of diffusional character. A special difficulty for the theoretical understanding of these processes stems from the mixture of (*a*) coherent dynamics on quantum mechanical potential surfaces, (*b*) collective motion of many degrees of freedom in the first solvation shell, and (*c*) diffusive dynamics on free-energy surfaces.

Ultrafast chemical reactions are often associated with conical intersections, which, albeit known for many decades (21, 22), have been largely overlooked until quite recently (23). Unlike the intersection of two one-dimensional potential curves of equal symmetry, which results in an avoided curve crossing, an intersection in two or more dimensions leads to a funnel-like region in the potential energy surface. Such a conical intersection permits crossing from the upper to the lower electronic state on an ultrafast timescale. In the resulting non-Born-Oppenheimer dynamics, vibrational and electronic degrees of freedom are strongly coupled, and hence the course of the reaction sensitively depends on the fine-tuning of the potential curves due to solute-solvent interactions and temperature effects, for example. Depending on the coupling to external degrees of freedom, a vibrational wave packet may be enabled or hindered to overcome a small barrier and to enter the active region of a conical intersection situated close to the Franck-Condon active region of the excited state.

Along with their direct impact on photoinduced reactions, all these phenomena tend to increase the complexity of the experimental data. This creates difficulty for the photochemist in separating out the contributions of the different relaxation processes as vibrational cooling and solvent relaxation from the intrinsic population dynamics. With well-separated timescales, changes in transient spectral signatures can safely be attributed to a specific process. Furthermore, the experimental results do not depend on the choice of the excitation wavelength. This is not true for the domain of ultrafast spectroscopy.

Commonly used techniques to study ultrafast photochemical processes are so-called population spectroscopies, such as transient absorption (24) and fluorescence upconversion (25), which monitor the population of excited states and the evolution of their spectral signatures as a function of time. The latter method of course can be applied only to fluorescing species. However, the obtained data are often more easy to interpret as only the population of the emitting state is probed, whereas with transient absorption, the sum of excited-state emission, excited-state absorption, and ground-state bleaching is recorded. Hence it is often difficult to disentangle the corresponding strongly overlapping contributions.

Technically more demanding are coherence spectroscopies such as the photon-echo techniques. Being sensitive to the fluctuating environment of electronic transitions and to couplings between nearby chromophores, they can be used to study relaxation processes of the solvent around a chromophore and to monitor chromophore-chromophore interactions on an ultrafast timescale (26, 27). Transient two-dimensional spectroscopy in the visible and infrared (IR) spectral domain can reveal such couplings and interactions in a fashion similar to two-dimensional NMR spectroscopy, monitoring the dephasing of coupled electronic transition dipoles instead of nuclear spins (28, 29).

Conical intersection: point where two potential energy surfaces of equal symmetry are degenerate and intersect each other

Wave packet: propagating wave function resulting from the coherent superposition of stationary wave functions

Vibrational cooling: heat transport from thermalized intramolecular low-frequency modes to the solvent via vibrational coupling

2. VIBRATIONAL RELAXATION

The Franck-Condon window of the excitation step often dictates that the upper state may be populated only with some excess vibrational energy. Furthermore, fast internal conversion upon photoexcitation may convert part of the electronic excitation energy into vibrational energy by means of a radiationless vibronic transition. Initially localized mainly in high-frequency modes,

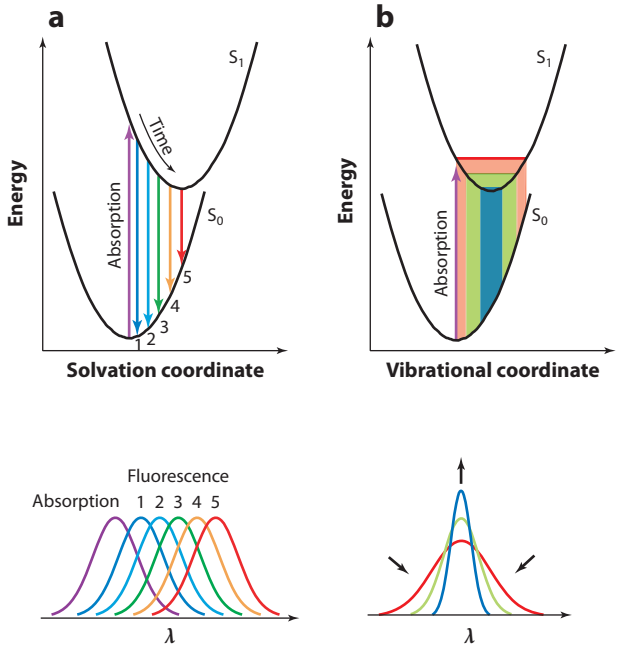

Figure 2

Schematic representation of typical spectral signatures associated with (*a*) solvation dynamics and (*b*) vibrational cooling. (*a*) Owing to the Franck-Condon principle, the electronic excited state is populated out of equilibrium. Subsequent solvent reorganization leads to a dynamic red shift of the emission band. (*b*) The excess vibrational energy leads to a broadening of the emission at early times. After vibrational cooling, the emission band sharpens.

this energy is quickly redistributed into the low-frequency part of the vibrational manifold through anharmonic coupling. This process, called intramolecular vibrational redistribution (IVR), leads eventually to a thermally distributed population in the low-frequency modes and permits one to attribute an internal vibrational temperature to the molecule. Intermolecular vibrational relaxation, so-called vibrational cooling, involves the coupling of solute and solvent vibrational modes. The energy in the solute's nuclear degrees of freedom is transferred to the molecular units in its first solvation shell from which it is dissipated into the bulk.

Excited vibrational states tend to be more extended in space compared to the vibrational ground state and open up new Franck-Condon windows around their turning points. A nonzero population in excited vibrational levels of an electronically excited state therefore tends to broaden transient absorption and emission bands in the visible spectral domain (**Figure 2**). Pigliucci et al. (16) reported the vibrational relaxation of substituted perylenes in different solvents and observed timescales for the spectral narrowing of a few hundreds of femtoseconds to a few picoseconds. Furthermore, they found that specific solute-solvent interactions such as hydrogen bonding and resonance conditions for low-frequency vibrational modes have a stronger influence on cooling than macroscopic solvent parameters such as the thermal diffusivity do.

It is often stated that IVR occurs prior to vibrational cooling because the intramolecular anharmonic coupling is supposed to be stronger than the coupling to solvent modes, the latter process having been described by means of unspecific pair-impact interactions (30). Strictly speaking, the term vibrational cooling already implies that IVR is complete and an internal temperature has been established before intermolecular vibrational relaxation starts. Indeed, for larger molecules,

Anharmonic coupling: coupling between different vibrational modes that would vanish in a harmonic normal-mode approximation; because of the anharmonic nature of the corresponding potential curves, the coupling is nonzero

Intramolecular vibrational redistribution (IVR): intramolecular redistribution of initial excess energy from high- to low-frequency vibrational modes through anharmonic coupling

vibrational relaxation times ranging from tens to a few hundreds of femtoseconds have been reported, whereas vibrational cooling typically takes place between one and several picoseconds (15, 31). However, the above-mentioned study on substituted perylenes (16) has revealed that vibrational coherences may survive on timescales at which vibrational cooling by the solvent is already fully active, suggesting that the latter can take place in parallel with IVR. Furthermore, the speed of intermolecular vibrational relaxation seems to correlate with the magnitude of the overlap integral between solute and solvent vibrational spectra, rather than correlating with macroscopic parameters such as viscosity or thermal conductivity.

RTIL: room-temperature ionic liquid

The population in low-frequency vibrational modes tends to downshift frequencies in the vibrational states through anharmonic coupling. In transient mid-IR experiments, one commonly observes red shifts and band broadenings on the red edge of the corresponding transient signals. A special case occurs with ultrafast photocycles in which larger amounts of energy are released to the vibrational manifold of the electronic ground state within a few picoseconds after excitation. Hamm and coworkers (32) demonstrated how to estimate the heat release to a reaction product by comparing measured band shapes with simulations based on knowledge of the anharmonic couplings. The spectral signature of the hot ground state has been used to estimate the amount of heat release and to track the pathway of ultrafast photochemical reactions (33). Interestingly, the band shapes due to hot ground-state populations obtained in these two publications closely resemble each other, despite the quite different molecular system. This seems to justify the assumption of attributing an internal temperature to a chromophore at timescales as short as 1 ps as long as the energy is simultaneously released to a large-enough distribution of low-frequency modes.

Substantial work still needs to be done before a comprehensive picture of the vibrational relaxation in liquids is obtained. Detailed knowledge on how vibrational energy is dissipated into the solvent would allow the possibility of influencing the dynamics or the outcome of a photochemical reaction by varying the excitation energy.

3. SOLVATION DYNAMICS

Along with the intramolecular degrees of freedom, there is in general a contribution from solvent relaxation to be observed as well. Following the same Franck-Condon principle as above, the orientation of the solvent molecules in the chromphore's first solvation shell right after excitation still corresponds to the equilibrium configuration of its ground state. In subsequent relaxation processes on timescales ranging from tens of femtoseconds to hundreds of picoseconds and even nanoseconds, depending on viscosity, the solvent molecules adapt their configurations toward the equilibrium of the excited state (**Figure 2**). As far as timescales are concerned, one distinguishes the so-called inertial response on a timescale of a few tens to a few hundreds of femtoseconds and the subsequent collective motion with diffusive character. The latter scales with the solvent's viscosity and may adopt average values from a few hundreds of femtoseconds in low-viscosity solvents such as water and acetonitrile to several nanoseconds in highly viscous liquids such as room-temperature ionic liquids (RTILs). The corresponding kinetics are in general highly nonexponential (14).

Two general types of solvation dynamics can be distinguished: polar or dielectric and nonpolar solvation. Nonpolar solvation involves mainly center of mass motion of the solvent molecules. Skinner and coworkers (34) developed a molecular theory that provides a microscopic foundation of Kubo's (35) stochastic theory of lineshapes in nonpolar media. Berg (36) has elaborated a viscoelastic continuum model based on the solvent's shear and compression moduli and their relaxation times. Upon ultrafast photoexcitation and the corresponding instantaneous change in size and shape of the solute's electronic cloud, the solvent cavity adapts itself first by coherent and subsequently diffusive motion. It is important to note that the first coherent or inertial part

within this model results from the finite, quantized mass of the particles in the vicinity of the solute. The corresponding inertia of the solvent molecules in the first solvent shell is responsible for the inertial dynamics, not their molecular structure. Treating the solvent mainly as an elastic and viscous continuum, the dynamic features of nonpolar solvation can be modeled down to a timescale of approximately 100 fs. Effects due to the finite particle size in the regime of the inertial motion on a sub-100-fs timescale are beyond the limits of a continuum theory. Based on this work, Berg and colleagues (37) applied the model to the vibrational echo of myoglobin-CO and discussed the relation between viscosity and the dynamics in the time range of spectral diffusion. Bagchi and coworkers (38) pointed out the close relation between nonpolar solvation dynamics and vibrational cooling in the case of strong solute-solvent interactions. A molecular theory of three-pulse photon echoes in nonpolar fluids was also elaborated on by Everitt & Skinner (39). Fleming and coworkers (40) compared results of their three-pulse photon-echo peak-shift experiments on a quadrupolar solute in different polar and nonpolar solvents with the above-mentioned viscoelastic models and found three distinct timescales: a sub-100-fs component attributed to inertial motion, a slower 2–3-ps component attributed to structural relaxation, and an intermediate timescale of approximately 600 fs of uncertain origin.

Van der Zwan & Hynes (41) pioneered the theoretical treatment of dielectric relaxation processes and introduced the term time-dependent dielectric friction. Their work has triggered a large number of experimental studies. The dielectric response of the solvent, treated as a continuum, leads to the well-known dynamic Stokes shift, which provides straightforward access to the timescales of solvent relaxation. In contrast to nonpolar solvation, polar solvation is mainly induced by the torque motion of polar molecules or moieties, which adapt the direction of their dipoles to the changed reaction field. Maroncelli and coworkers (14) undertook an extensive experimental study of polar solvation, measuring the temporal evolution of the fluorescence emission of coumarin 153 in a long list of solvents of different polarity and viscosity by fluorescence upconversion. More recently, different authors reported on dielectric solvation dynamics observed in ionic liquids with surprisingly differing results (25). A major experimental problem with the upconversion technique, in which the time-resolved emission spectrum has to be reconstructed from single-wavelength kinetics, is the need to calibrate the relative signal intensities over the observation window. The amplitudes of the early time features relative to the bulk of the diffusive relaxation rely on the accuracy with which the steady-state emission spectrum can be recorded in its outer blue wing. Any distortion due to reabsorption, small impurities, and nonflatness of the detector response, for example, can significantly alter the results. Hence differences as large as half an order of magnitude between different publications can be found (25). Ernsting and coworkers (24, 25) used transient absorption and ultrabroadband fluorescence upconversion to decompose the experimental data into different contributions and to isolate the solvent response part on the early timescale.

The various photon-echo techniques allow both nonpolar and polar solvation dynamics to be addressed without the need of fluorescent probes. Whereas population spectroscopies such as transient absorption and fluorescence upconversion record the evolution of the transition frequency averaged over the sample (the so-called Stokes-shift correlation function), coherent spectroscopies monitor the diffusive motion of the transition frequency of the individual molecules within the corresponding band. Its average over the ensemble is called the system-bath correlation function. Within the regime of linear solvent response, these two correlation functions are tightly linked via a Kramers-Kronig relation (42), the so-called fluctuation-dissipation theorem. Hence the correlation functions obtained from the dissipative (population) and dispersive (coherence) dynamics should essentially be the same. Wiersma and coworkers (43) as well as Fleming & Cho (44) worked out this principle from the theoretical side and demonstrated experimentally a match

between the different approaches within an order of magnitude; however, for technical reasons, different solvation probes were used for the different methods. A systematic comparison under identical experimental conditions still needs to be done.

Over the past few years, RTILs have gathered much interest. Solvation dynamics in RTILs has been studied by various groups with surprisingly differing results (25). Using broadband fluorescence upconversion and time-correlated single-photon counting, Maroncelli and coworkers (45) covered the range from 100 fs to 10 ns and showed that dielectric solvation in RTILs is systematically slower by a factor of three to five compared to predictions from conventional continuum models.

OKE: optical Kerr effect

MBO: multimode Brownian oscillator

The optical Kerr effect (OKE) and terahertz spectroscopy can be used to investigate vibrational and rotational dynamics in neat solvents. For instance, Turton & Wynne (46) measured the OKE in a wide variety of liquids, from simple rare gas fluids and globular-molecular liquids to aqueous salt solutions, water, and RTILs. Whereas inhomogeneities and corresponding complex dynamics in strongly interacting liquids such as water and RTILs are to be expected, the occurrence of similarly complex dynamics in noble gas fluids is surprising and may be linked to findings on nonpolar solvation dynamics, for which even a single reaction coordinate may induce dynamics on multiple timescales (36).

The multitude of different intra- and intermolecular relaxation processes typically occurring on the femtosecond and picosecond timescales has been successfully described in many cases by means of the phenomenological multimode Brownian oscillator (MBO) model (27, 47, 48). The physical observables of the experimental approaches in ultrafast spectroscopy are mostly the amplitude and frequency of an optical transition coupled to a bath of vibrational modes. The primary solvation coordinate of the two-level system is modeled using a displaced harmonic oscillator in which the displacement depends on the dynamics in the various degrees of freedom. The MBO model establishes an elegant way to incorporate the full range from coherent quantum dynamics to diffusive classical and collective dynamics within a single model.

Book & Scherer (49) studied the influence of intramolecular vibrational dynamics on electronic dephasing using the MBO model. Lazonder & Pshenichnikov (50) discussed the temperature dependence of the optical response in glass-forming liquids within the framework of the MBO model. The obtained modes are tested over a wide temperature range by freezing out parts of the bath oscillations. Fleming and coworkers (51) investigated the protein dynamics of bacteriorhodopsin using photon-echo and transient absorption spectroscopy and found that the experimental results can be simulated using the MBO formalism. They found that only a small number of modes representing known vibrations of the retinal are required to reproduce the experimental data and concluded that the response of the retinal is only inertial because of the covalently constrained, polymeric nature of the protein. Giraud and Wynne (42) pointed out the link between solvation dynamics and the corresponding IR and Raman lineshapes. They used the parameters obtained from a fit to OKE data to simulate the corresponding IR and Raman lineshapes. Ultrafast solvation dynamics in pyrrolidinium ionic liquids has been investigated by Shirota et al. (52). Fitting MBO-based lineshapes to the experimental data reveals three different timescales of the order of 2 ps, 20 ps, and 200 ps to 3 ns, with the last one scaling with viscosity.

It has, however, been pointed out that even solvation dynamics involving only a single solvent coordinate can produce multiple timescales, provided the dynamics on this coordinate is sufficiently complex (36). Accordingly, the link between the response in the frequency domain and the dominant solvent modes can be complicated.

Even though there has been an extensive amount of research by many groups over the past two decades, the level of understanding of dynamic solvation processes remains somewhat qualitative. The technical limitations of the experimental setups employed until recently still prevent us from

reliable comparisons with theoretical models on a detailed quantitative level. The recent improvements in broadband detection with quantitative photometric resolution (25) will hopefully bring the community a step forward toward an understanding of solvation dynamics that permits not only the prediction but also the fine-tuning of the outcome of ultrafast photochemical reactions.

ET: electron transfer

CS: charge separation

CR: charge recombination

Nonadiabatic process: process involving the jumping from the reactant to the product energy surface

4. ELECTRON TRANSFER

Electron transfer (ET) can be considered to be the most simple chemical reaction as it involves only the displacement of the smallest chemically relevant particle from one molecular moiety, the donor, to another, the acceptor (53, 54). This is also why these processes are probably the fastest chemical reactions. Indeed, an ET does not involve bond formation or breaking but only some reorganization of intramolecular and/or solvent coordinates. Here we mainly address photoinduced charge separation (CS), i.e., ET between two neutral reactants, and charge recombination (CR), i.e., the decay of the CS product back to the neutral reactant state. As both photoinduced CS and CR are key steps for important applications (55, 56), such as photovoltaics and artificial photosynthesis (57–59), they have been intensively investigated over the past four decades (60, 61). Experimentally, the dynamics of photoinduced CS can be studied by measuring the fluorescence decay of the excited reactant. Alternatively, transient absorption can be used to monitor the decay of the excited reactant and/or the build up of the CS state population. However, the CS product often does not fluoresce, and thus the investigation of the CR dynamics is usually performed by transient absorption.

ET reactions with weak to moderate free energy (i.e., $-\Delta G_{ET} \leq \sim 1 - 1.5$ eV) are usually discussed within the framework of the classical Marcus theory as thermally activated processes (62). In this model, thermal fluctuations of some relevant intramolecular/solvent modes, which constitute the reaction coordinate, bring the reactant to a configuration in which its free energy matches that of the product. ET proceeds then by tunneling, and relaxation brings the product state to thermal equilibrium. The classical barrier between reactant and product states decreases with increasing ET driving force, until it vanishes. As a consequence the ET rate constant, k_{ET}, increases with the driving force. This is the so-called normal region. For highly exergonic reactions, ET is better described as a nonradiative transition, and k_{ET} can be expressed in terms of a Fermi golden rule equation (62, 63):

$$k_{ET} = \frac{2\pi}{\hbar} V^2 \cdot FCWD, \quad (1)$$

where V is the electronic coupling between the reactant and product states, and $FCWD$ is the Franck-Condon weighted density of states. The latter term is responsible for the decrease of k_{ET} with the increasing energy gap between reactant and product states, the so-called Marcus inverted region. ET is thus the fastest at the turning point between the normal and inverted regions, in the so-called barrierless regime. Over the past four decades, there have been many experimental investigations on the driving-force dependence of the ET dynamics to verify these theoretical predictions. The inverted regime has been reported for many different types of ET processes, such as inter- (64, 65) and intramolecular CR (66) and charge shift (67), and intramolecular photoinduced CS (68), but there is still no convincing evidence of this regime for bimolecular photoinduced CS. Here, instead of decreasing, k_{ET} remains essentially constant and equal to the diffusion limit (69). The origin of this discrepancy is still debated (70, 71). Equation 1 is valid only for nonadiabatic ET, i.e., where V is sufficiently small so that, once the system has reached the crossing point of the reactant and product free-energy curves, the transfer probability is much smaller than one. Thus, in the barrierless regime, the ET rate depends only on this curve-jumping process. Typical ET time constants in this regime are of the order of a few picoseconds. In many cases,

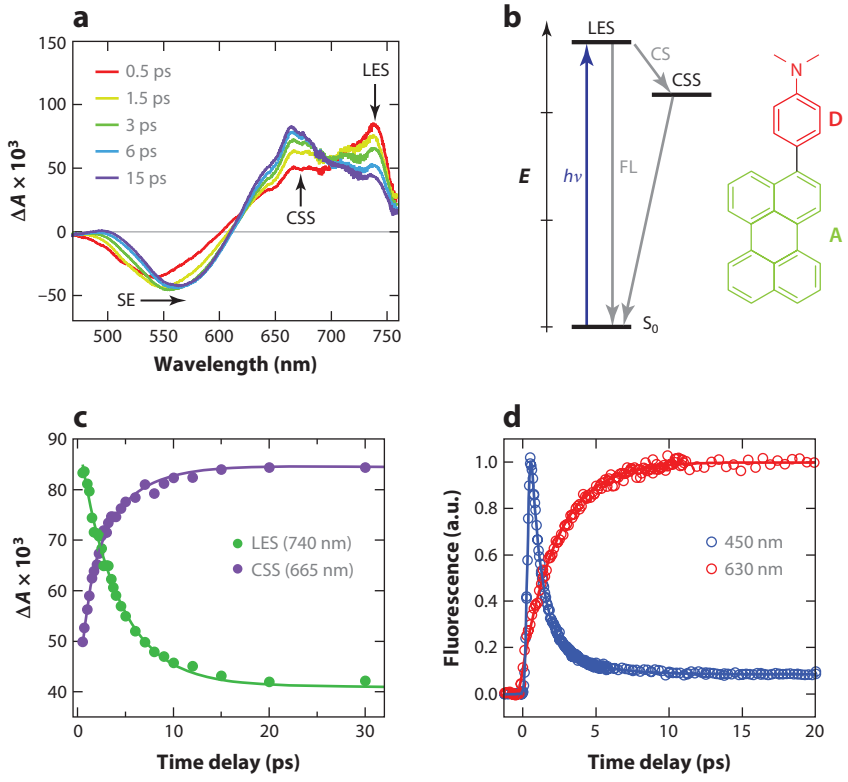

Figure 3

(*a*) Transient absorption spectra recorded at different time delays after 400-nm excitation of CNPeDMA (*b*) in THF, illustrating the decay of the locally excited-state (LES) population, the build up of the charge-separated state (CSS) population, and the shift of the stimulated emission band. (*c*) Time profiles at the maxima of the two transient bands. (*d*) Time profiles measured by fluorescence upconversion at wavelengths corresponding to LES and CSS emission. Here the dynamics not only reflects the CS, but also reflects the solvent relaxation of both the LES and CSS.

the time constants of ultrafast ET processes are found to correlate with the relaxation time of the solvent in which the reaction takes place (72–74). This is, for example, the case with 3-(*p-N,N*-dimethylaminophenyl)perylene (PeDMA) (**Figure 3**) for which intramolecular CS from the dimethylaniline to the excited perylene units takes place with time constants of approximately 700 fs, 2.2 ps, and 72 ps in acetonitrile, DMSO (dimethylsulfoxide), and 1-butanol, respectively, whereas the average solvation times, τ_s, amount to 260 fs, 2 ps, and 103 ps (75). However, CS in PeDMA does not take place in apolar solvents. This dynamic solvent control of ET has been theoretically explained by the fact that all but the reaction coordinate are in quasi-equilibrium during the ET process (76, 77). Therefore, the evolution of the system along the reaction coordinate in principle cannot be faster than vibrational and solvent relaxation. Depending on the relative magnitudes of V and τ_s, the rate-limiting step in ET is thus no longer the curve jumping accounted for by V, but the evolution along the reaction coordinate toward the crossing region, determined by τ_s (76, 77). In other words, if solvation is required to make ET energetically feasible, ET cannot be faster than solvation. As discussed above, solvent relaxation exhibits multiphasic dynamics, and thus partial solvation might suffice to make ET operative (74). This has been observed, e.g., with 3-cyano-10-(*p-N,N*-dimethylaminophenyl)perylene (CNPeDMA), for which the presence of a

PeDMA: 3-(*p-N,N*-dimethylaminophenyl) perylene

CNPeDMA: 3-cyano-10-(*p-N,N*-dimethylaminophenyl) perylene

CT: charge transfer

TCNE: tetracyanoethylene

CN group on the perylene moiety increases the CS driving force (75). In this case, the CS time constants amount to 180 fs and 480 fs in acetonitrile and DMSO, i.e., are faster than the average solvation time but still slower than the fastest solvation components that amount to 90 and 210 fs, respectively.

Well-known cases of CS faster than diffusive solvation involve the quenching of excited chromophores such as Nile blue or coumarins in electron-donating solvents, mostly anilines (78, 79). Typically, the fluorescence decay of the excited acceptor is found to be nonexponential with a dominating ~100-fs component. Conversely, the diffusive solvation time of anilines is of the order of 10 ps (80). ET faster than solvation can be explained using the Sumi-Marcus model (81, 82), which partitions the reactive coordinates into slow and fast ones. The former are mostly related to diffusive solvation, whereas the latter are associated with inertial solvation or intramolecular modes. In this model, the effective reaction path may differ from the minimum free-energy path if it leads more rapidly to the product. Therefore, the reaction may proceed along a pathway in which the slower coordinate is not fully equilibrated as long as the barrier toward the product is not too high.

ET faster than solvation has also been observed in CR of ion pairs, produced upon direct excitation in the charge transfer (CT) band of DA complexes (83–85). For example, the CR time constant measured upon CT excitation of the trimethoxybenzene/tetracyanoethylene (TCNE) complex is shorter than 100 fs and 140 fs in acetonitrile and valeronitrile, whereas the diffusive solvation time amounts to 260 fs and approximately 4 ps, respectively (84). This indicates that CR occurs in parallel to solvent relaxation, i.e., before solvent stabilization of the ion pair is complete. A consequence of this nonequilibrium dynamics, which can be discussed in terms of a semiclassical variant of the Sumi-Marcus model (82), is that the driving-force dependence of the CR rate constant is no longer bell shaped. Instead, the logarithm of the rate constant increases almost linearly with decreasing driving force, and there is no normal region to be observed (83, 86). This absence of the normal regime arises from the fact that the ion pair population efficiently recombines before reaching equilibrium from which CR would be thermally activated. Another interesting effect is that the CR dynamics of ion pairs produced by direct CT excitation may depend on the excitation wavelength. This effect, predicted theoretically (87, 88), has been experimentally verified with various DA complexes in polar solvents with a diffusive solvation time of a few picoseconds (84, 89). Excitation on the red edge of the CT band resulted in close to exponential CR dynamics, whereas, upon shorter wavelength excitation, the CR dynamics was found to be slower and nonexponential, with a rate increasing with time (**Figure 4**). In the latter case, the ion pair state is produced further away from equilibrium, and thus some relaxation is required before the system reaches a region at which the Franck-Condon factor for CR is large enough to make CR faster than further solvent relaxation.

Nonequilibrium CR dynamics has also been observed for ion pairs generated upon ultrafast bimolecular photoinduced CS. Whereas conventional ET theory predicted slow CR in agreement with the normal regime, CR rate constants faster by more than three orders of magnitude were observed (13, 90). Such effects had been largely overlooked before because of the insufficient temporal resolution of the experimental setup. Of course, these nonequilibrium effects take place only if V is large enough so that the ET dynamics is not controlled by the state-hopping probability.

Clearly, intramolecular modes play a crucial role in ET reactions. As vibrational dephasing in the condensed phase can take several picoseconds, the possibility of observing coherent photoinduced ET processes upon ultrashort optical excitation has been investigated (91, 92). Evidence of such an effect has been obtained by Hochstrasser and coworkers (12) upon direct CT excitation of a pyrene/TCNE DA complex in solution. The transient absorption profiles at wavelengths corresponding to the decay of the ion pair population and to the recovery of the ground-state

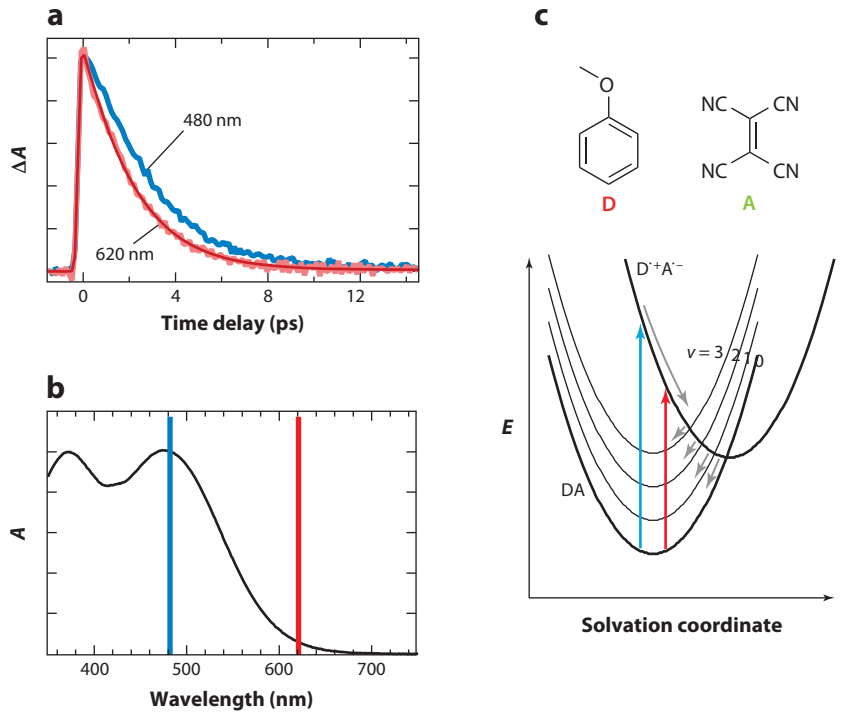

Figure 4

(*a*) Time profiles of the transient absorption measured upon photoexcitation at two different wavelengths (480 and 620 nm) in the absorption band of the anisol/TCNE donor-acceptor complex in octanenitrile (*b*). The transient absorption signal results from $TCNE^-$, and the decay reflects the charge recombination of the ion pair state D^+A^-. As charge recombination occurs during the relaxation of the ion pair state, its dynamics depends on how far from equilibrium this state has been initially populated (*c*).

population exhibited a periodic oscillation typical for a vibrational wave packet. The authors concluded that the vibrational coherence observed in the ground-state recovery dynamics resulted not only from stimulated Raman scattering, but also from the coherent repopulation of the ground state by CR. Similar oscillations due to vibrational wave-packet motion were later observed in the CT emission of various excited DA complexes (19, 93). The oscillation frequency was found to depend only on the electron acceptor (e.g., TCNE, fluoranil, and chloranil), not on the donor, and was assigned to an out-of-plane bending mode of the acceptors.

Indications of the involvement of vibrational coherence in ET have also been reported for the photoinduced bimolecular ET quenching of oxazine in a pure electron-donating solvent (94). Periodic oscillations due to vibrational wave-packet motion were found in the transient absorption profiles of the excited-state and ground-state populations. Despite detailed theoretical simulations of the experimental data, evidence of coherent CS could not be firmly established (95). Further investigations by the same group revealed the presence of wave-packet motion on the transient absorption profile of the CS product as well, pointing to the importance of vibrational dynamics on the reaction (96).

Despite these investigations, the effect of vibrational coherence on the dynamics of ET processes in liquids is far from being fully understood. Further studies on the effect of selective vibrational excitation on the dynamics of ultrafast ET processes are required before a clear picture

can be obtained. Of course, in parallel to this, a more detailed understanding of the dynamics of vibrational relaxation in liquids is also needed.

PT: proton transfer

ZPE: zero-point energy

Adiabatic process: process occurring on a single energy surface

ES(I)PT: excited-state (intramolecular) proton transfer

5. PROTON TRANSFER

Similar to ET, proton transfer (PT) reactions constitute elementary steps of important and relevant processes in fields as diverse as chemistry, physics, and biology, while still being among the simplest possible reactions. The apparent similarity of ET and PT has triggered various theoretical descriptions. Marcus (97) obtained a similar expression as for ET reactions, with the most important difference being the absence of an inverted region as long as the reaction coordinate mostly results from bond rupture bond formation. Agmon & Levine (98) derived a free-energy relationship introducing a mixing entropy, which accounts for the activation barrier, and can adequately reproduce kinetic isotope effects for PT reactions. Eventually, Kiefer & Hynes (99) established that the activation free energy of PT is, similar to the Marcus description of ET, largely determined by the reorganization of the surrounding polar solvent and the zero-point-energy (ZPE) changes associated with the quantum nature of the proton. This is in marked contrast to the above approaches, for which the proton coordinate is the reaction coordinate. These authors distinguished two extreme cases of PT (100). First, in adiabatic PT, the proton is treated quantum mechanically, but no proton tunneling is involved. The latter is a consequence of the fact that the proton ZPE lifts the lowest vibrational level above the PT barrier once the solvent has rearranged. Second, in nonadiabatic PT, in which the two lowest vibrational energy levels of the mode associated with PT fall below the potential barrier, the PT reaction takes place exclusively via tunneling. Given the short tunneling length of PT reactions (25 to 35 $Å^{-1}$), low-frequency molecular vibrations can modulate the PT DA distance and thus the coupling, eventually enhancing the observed PT reaction rates (101). These oscillations may also be at the origin of spurious observations of the inverted regime in PT reactions (102, 103). In fact, recent theoretical studies indicate that for PT (and proton-coupled ET), an inverted regime cannot be observed by a simple variation of the driving force (104).

Apart from a few exceptions (105), there has been limited experimental access to the dynamics of PT reactions in the electronic ground state. However, excited-state PT (ESPT) reactions have gained significant importance in serving as model systems for fundamental chemical reactions (106, 107) as well as in living systems (108–110). As such reactions can be easily triggered by optical pulses, their dynamics can be precisely monitored (111). Photoacidity, i.e., the increased acidity of certain substances in the electronically excited state (112), has been successfully applied to perform pH jump experiments and thus to monitor proton-driven chemical phenomena, such as protein folding, in real time (113–115).

One may visualize two different scenarios for ESPT, in which the proton donor and acceptor reside either within the same molecule (intramolecular ESPT) or in different molecular entities (bimolecular or, if one of the reactant partners is the solvent itself, pseudounimolecular ESPT). Leaving aside the additional complications arising with intermolecular PT reactions (see the sidebar, Diffusional Effects on Ultrafast Intermolecular Reactions), we now briefly look at ultrafast intramolecular ESPT (ESIPT) reactions in simple organic model systems (**Figure 5**). Many of these reactions have been found to be solvent insensitive and to fall into the limit of barrierless adiabatic reactions, making ESIPT as fast as 30 to 100 fs (5–8). In addition, the presence of oscillations due to vibrational wave packets in the observed time profiles allowed the identification of low-frequency deformations of the molecular skeleton, hosting the proton donor and acceptor, relevant for ESIPT. By comparing deuterated and nondeuterated HBT [2-(2′-hydroxyphenyl)benzothiazole], Riedle and coworkers (8) found no kinetic isotope effect,

DIFFUSIONAL EFFECTS ON ULTRAFAST INTERMOLECULAR REACTIONS

Passing from intra- to intermolecular ultrafast processes adds a level of complexity to the interpretation of experimental data. In addition to the aforementioned nonequilibrium population in the internal and external degrees of freedom realized upon optical excitation, the mutual reactant material transport is also not equilibrated. Consequently, the rate coefficients observed just after excitation of one of the reactants are time dependent (**Figure 6**), leading to the appearance of a nonexponential decay of the reactant population, the so-called transient effect (169–171). Consistent theoretical descriptions of these phenomena require the use of diffusion-reaction equations. By doing so, we can properly account not only for the mutual reactants' diffusion, but also for the specificities of the reaction itself, such as its distance and free-energy dependence. This approach has been successfully applied to irreversible photoinduced bimolecular ET (17, 172, 173), PT between photoacids and bases (111, 174), and reversible bimolecular PT from photoacids to the solvent and subsequent geminate recombination of the proton/conjugate base pair (111, 175).

thus excluding proton tunneling as the main reaction step. Instead, in line with previous findings on HBQ (10-hydroxy-benzo[h]quinoline) by Takeuchi & Tahara (7), the involvement of low-frequency skeletal deformations and the resulting ballistic wave-packet trajectory on the multidimensional potential energy surface were identified as rather general features of intramolecular PT for these types of molecules. In another study, Waluk and coworkers (116) found that in PI [7-(2-pyridyl)-indole] the ultrafast barrierless PT is governed by a large-amplitude phenyl twist rather than by low-amplitude skeletal motions.

Another interesting system is AI (7-azaindole), which can undergo intermolecular double PT in its dimeric state, thus mimicking DNA base pairs and their associated PT dynamics (117, 118). Here, the double PT is found to be strongly solvent-polarity dependent and to proceed in a nonconcerted fashion, i.e., forming an intermediate ionic species (118).

Often the transfer of a proton is significantly influenced or even triggered by a preceding or parallel transfer of an electron between the PT reaction partners. These so-called proton-coupled electron transfer (PCET) reactions, in which a proton and an electron are transferred either

Transient effect: time dependence of the rate constant of a bimolecular reaction due to nonequilibrium reactant pair distribution

PCET: proton-coupled electron transfer

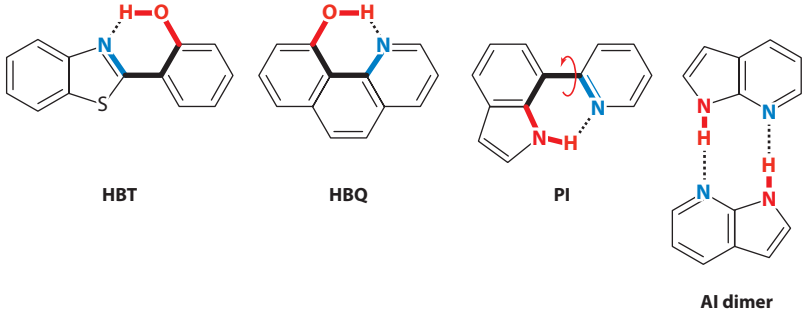

Figure 5

Structures of molecules exhibiting excited-state intramolecular proton transfer. The normal form has the proton residing on the red functional group and the tautomer on the blue. Abbreviations: HBT, 2-(2′-hydroxyphenyl)benzothiazole; HBQ, 10-hydroxy-benzo[h]quinoline; PI, 7-(2-pyridyl)-indole; AI, 7-azaindole.

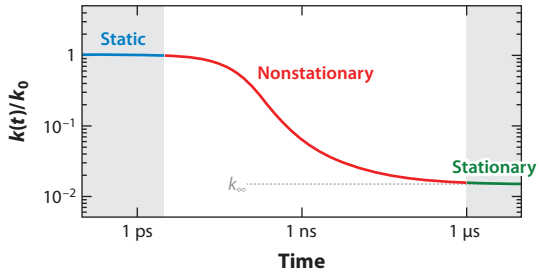

Figure 6

Time dependence of the bimolecular photoinduced electron transfer rate in solution. At early times, the reaction takes place between reactant pairs at an optimal distance with the intrinsic rate constant k_0. Once these pairs have reacted, the reaction occurs between pairs, which are increasingly more remote, and thus the rate decreases continuously until it becomes equal to the rate at which pairs are produced by diffusion, k_∞.

simultaneously or sequentially, have received considerable attention over the past three decades, from both experimental (119) and theoretical groups (120–122), owing to their importance in areas covering such diverse topics as photosynthesis (57), catalysis (123), and hydrogen production (124) or enzyme reactions (125). Here we emphasize only photoinduced PCET reactions, which are relevant for biological processes such as radiation-induced DNA damage (126) as well for the primary events in solar cells (127), and how nonequilibrium processes, triggered by the absorption of light, can affect them.

From a theoretical point of view, PCET reactions are significantly more complex to handle than their individual steps (i.e., ET and PT) (122). The overall PCET process can be dominated by both solute and solvent motion, the timescales of which (and hence those of PT and ET) can strongly vary. In addition, quantum effects, such as tunneling or ZPE, may become important, such as for the description of a pure PT (100). The extent of coupling between the electronic and vibrational states involved (either adiabatic or nonadiabatic), as well as the inclusion or exclusion of the proton quantum effects, allows a multitude of limiting cases to be distinguished for PCET reactions (128). To make things even more involved, the distances between both electron and proton DAs (which are not necessarily the same) can modulate the degree of coupling and thus lead to a distance-dependent transition between these different cases. By analogy to theoretical descriptions of ET rate constants (76), expressions for PCET rate constants have been derived by interpolating between Fermi golden rule and solvent control limits (129).

Another current challenge concerns the modeling of photoinduced PCET processes exhibiting highly nonequilibrium dynamics of both solute and solvent (130). As a consequence, the above-mentioned models for PCET have to be expanded to account for solvent and proton relaxation mechanisms. Hammes-Schiffer and coworkers (131) recently discussed two PCET model systems using multiple scalar solvent coordinates accounting for the ET and PT reactions, by including the dielectric constant, Debye relaxation times, and moments of inertia of the solvents as well as the relevant solute properties for the electron-proton free-energy surfaces.

The experimental studies on excited-state PCET reactions cover a wide range of systems, starting from relatively simple organic photoacids and super-photoacids (112), over PCET in paradigmatic metal-organic complexes involved in photosynthesis (132), to proton and ET in biomolecules such as green fluorescent protein (133).

We discuss two types of prototypic systems exhibiting photoinduced ET and PT to illustrate the complex and sensitive interplay of PT, ET, and nonequilibrium solvent dynamics (6, 134, 135). The molecule 3-hydroxyflavone (system 1 in **Figure 7**) undergoes an ultrafast (35 fs to 60 fs) PT that is almost completely solvent independent (136). However, as soon as an electron-donating

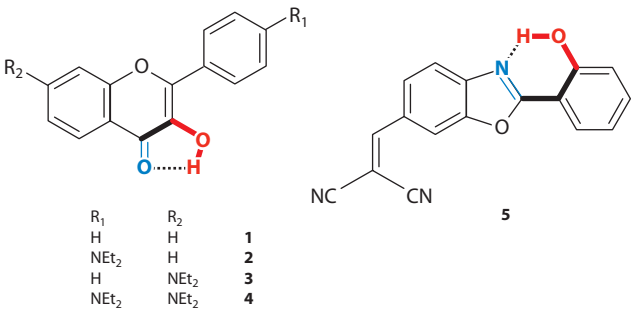

R_1	R_2	
H	H	**1**
NEt_2	H	**2**
H	NEt_2	**3**
NEt_2	NEt_2	**4**

Figure 7

Molecules exhibiting solvent-influenced proton-coupled electron transfer (135). The normal form has the proton residing on the red functional group and the tautomer on the blue.

group is introduced (system 2 in **Figure 7**), the excited-state dynamics changes drastically (135). Femtosecond-resolved fluorescence upconversion studies have revealed the following scenario: Excitation of the normal (ground-state) form populates a CT state, whose emission band exhibits a red shift in polar solvents due to solvent relaxation as a consequence of the difference of the electric dipole moment between the ground and the electronic excited states. The multiphasic rise of a new, strongly red-shifted emission band, which can be attributed to the ESIPT tautomer, is observed. The fastest ESIPT rate can be attributed to barrierless PT from the Franck-Condon state before solvent relaxation of the initially excited form starts. The stabilization of this state upon relaxation renders the ESIPT a solvent-polarity-dependent (i.e., slowing down with increasing solvent polarity) activated process (135). Analogous results were obtained for system 2 in **Figure 7** in RTILs and conventional solvents using optical Kerr gate fluorescence measurements, which allowed the quantitative decomposition of the time-resolved spectra and monitoring of the spectrotemporal evolution of the normal and tautomer forms (134). By varying the magnitude and direction of the dipole moment change between the ground and excited state of the normal forms (systems 2–4 in **Figure 7**), Chou and coworkers fine-tuned the observed PCET dynamics. Whereas systems 2 and 3 showed strongly solvent-polarity-dependent dual emission from both forms, the dipole cancellation due to the presence of the two opposing electron-donating moieties in system 4 led to solvent-polarity decoupled PT (135).

System 5, conversely, exhibits a fast concerted PCET, resulting in a "proton"- and "electron"-transferred excited state with significant nonequilibrium polarization (again the dipole moment is altered with respect to the ground state). Contrary to systems 2 and 3, the tautomer emission spectrum now exhibits a temporal red shift, indicative of solvent relaxation after PCET (135). At present, one of the crucial points consists of setting up a unified classification of P(CE)T reactions and properly characterizing them to enable comparison between experiment and theory. At the same time, considerable efforts toward the synthesis of simple paradigmatic molecules to model as many cases as possible are still necessary. Eventually, the existing and continuously growing arsenal of ultrafast spectroscopic techniques, especially those yielding structural information, should help to unravel the mechanism underlying these elementary processes.

6. PHOTOISOMERIZATION REACTIONS

Cis-trans isomerization is probably one of the simplest unimolecular chemical reactions that involves neither the transfer of a particle or a group of atoms nor the breaking or the formation of a bond. Whereas *cis-trans* isomerization around a double C=C bond is associated with a very large

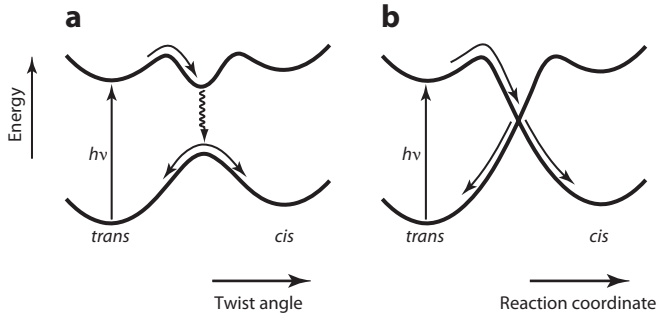

Figure 8

Potential energy profiles of the ground and excited states, illustrating *cis-trans* photoisomerization via (*a*) an avoided crossing and (*b*) a conical intersection. In panel *a*, only one coordinate (e.g., the C=C twist angle) is varied, whereas in panel *b*, at least two coordinates are involved.

activation energy in the electronic ground state, it can proceed essentially barrierless in a π-π^* excited state and, in such a case, can be ultrafast. The photoisomerization of the 11-*cis*-retinal to all-*trans*-retinal in rhodopsin is the primary step of vision and takes place on the subpicosecond timescale (10, 137, 138). The theoretical picture of the photoisomerization mechanism has evolved considerably over the past few decades (11). Originally, this reaction was modeled in a one-dimensional picture of the ground- and excited-state potential energies along the C=C twist angle (**Figure 8**). In this picture, the two energy curves do not intersect but undergo avoided crossing. The excited molecule twists around the C=C bond until it reaches the minimum of the upper potential energy curve, where the twist angle is between the *cis* and *trans* conformations and, once there, jumps nonradiatively to the ground-state curve, where it undergoes a further twist toward the product state or backtwist to the initial ground state (139–141). This picture with an avoided crossing between the ground and excited states was not fully consistent with the experimental results as, in several cases, the measured reaction rate constants were much faster than those predicted according to the energy gap law for nonradiative transitions (9, 142, 143). Moreover, there was no direct spectroscopic evidence of the existence of an intermediate state that corresponds to the minimum of the excited-state potential, the so-called phantom state. It is now well established that these photoisomerizations involve conical intersections between the excited- and ground-state potential energy surfaces that can be reached not only by a twist around the C=C double bound, but additionally by distorting at least another intramolecular coordinate (11, 144, 145). For example, quantum chemical calculations of the photoisomerization of stilbene indicated that pyramidalization at one of the ethylenic carbons is required, in addition to C=C double bond torsion, for the excited-state population to reach an S_1/S_0 conical intersection (146). Other evidence pointing to the involvement of several modes comes from the viscosity dependence of the isomerization dynamics. Indeed, the C=C bond torsion requires a relatively large-amplitude motion of a fragment of the molecule and should thus be substantially influenced by the frictional drag exerted by the environment. Consequently, these reactions have often been discussed within the framework of Kramers' theory of activated barrier crossing (147), which in the high-friction regime predicts the isomerization rate constant to be inversely proportional to friction and, if the latter is assumed to be hydrodynamic, to viscosity. This viscosity dependence has been observed in a few cases only. In most cases, the observed rate constant, k_{iso}, correlates with the viscosity, η, in a power law $k_{iso} \propto \eta^{-\alpha}$ with $\alpha < 1$ (148). This departure from $\alpha = 1$ has first been ascribed to the failure of the hydrodynamic model to account for the microscopic friction (149). There have been several semiempirical approaches to solve this problem, such as

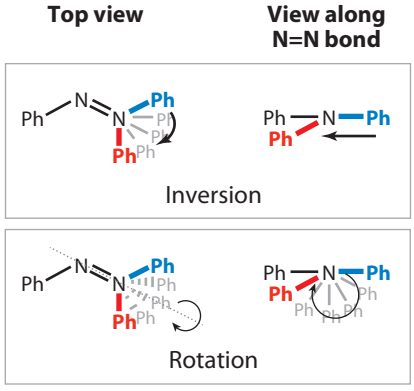

Figure 9

Comparison of the inversion and rotation mechanisms for the *trans-cis* isomerization of azobenzene and its derivatives. Inversion proceeds by changing the NNC angle, whereas rotation occurs by rotating the phenyl group about the N=N axis.

the Kramers-Hubbard model, in which local friction is deduced from the reorientational time of the molecule (150), or the use of the translational microviscosity calculated from the Spernol and Wirtz formula (151). Grote & Hynes (152) proposed an extension of Kramers' theory that accounts for the frequency dependence of friction. Although the experimental viscosity dependence of k_{iso} could be well reproduced with this model (153–155), the values of the best-fit parameters were not physically reasonable. This discrepancy was explained by the involvement of coordinates other than the double bond twist, which are not taken into account in these one-dimensional models. The introduction of additional coordinates allows isomerization without large-amplitude motion and can account for the weak viscosity dependence observed in some cases. For example, the so-called hula twist, which involves the simultaneous rotation around the C=C double bond and an adjacent C-C single bond (156), has been demonstrated for 2,2′-previtamin D and dimethylstilbene, which both undergo photoisomerization in low-temperature glasses (157, 158). Such a mechanism has also been invoked to account for the weak viscosity dependence of the photoisomerization of the green fluorescent protein chromophore in solution (159, 160), as well as for the ultrafast photoisomerization of retinal in the binding pocket of rhodopsin (156). In the latter case, such a concerted mechanism has been confirmed by femtosecond stimulated Raman spectroscopy (FSRS) (10).

Azobenzene and its derivatives constitute another important class of photoswitches with applications in biology (161), use in molecular motors (162), or light-driven switching devices (163). Unlike stilbene, azobenzenes have two possible mechanistic pathways for *trans-cis* isomerization, namely the stilbene-like rotation around the central N=N double bond and inversion about one of the two nitrogen atoms (164). Whereas initial experimental observations pointed toward a rotational mechanism upon $S_2 \leftarrow S_0$ excitation and an inversion mechanism for $S_1 \leftarrow S_0$ excitation (32, 165), recent structural investigations using either FSRS or time-resolved photoelectron spectroscopy point toward inversion as the dominant mechanism under all excitation conditions (166, 167). Using FSRS, Hoffman & Mathies (168) proposed the following isomerization mechanism for a DA substituted azobenzene derivative (**Figure 9**). Initially, CNN angle bending (inversion) leads to a bifurcation, in which a small portion of the population continues undergoing CNN bending as well as additional phenyl torsional motions [along the CCNN, CNNC (rotation), and NNCC bonds] to give the *cis* product within 800 fs, while the remainder of the population

FSRS: femtosecond stimulated Raman spectroscopy

bends back along CNN, yielding the vibrationally hot ground state of the *trans* state (after 2–3 ps). This latter investigation shows that the continuous improvement and development of novel spectroscopic and theoretical tools will probably lead to a comprehensive understanding of the mechanisms underlying these ultrafast processes.

SUMMARY POINTS

1. IVR and solvent relaxation often influence or even control the outcome of photochemical reactions. The present level of understanding of the involved coupling mechanisms and timescales needs to be refined by means of systematic studies with improved quality of experimental data.
2. The origin of the differences in experimental results on the Stokes-shift correlation function obtained in different laboratories has to be identified and the quality of experimental data improved to be able to quantitatively test fundamental assumptions, such as the validity of the regime of linear response for particular solvents and the applicability and limits of continuum models for solvation dynamics.
3. Photoinduced ET reactions can take place on similar or even shorter timescales than solvent and vibrational relaxation. In this case, the observed dynamics deviates from exponentiality and can depend on the excitation wavelength.
4. The effect of vibrational coherence on ET reactions still needs further investigation.
5. Barrierless PT reactions can be as fast as tens of femtoseconds.
6. There are several mechanisms for proton-coupled ET reactions. Depending on the structure and dynamic properties of solutes and solvents, ET can precede, accompany, or follow PT.
7. *Cis-trans*-type photoisomerization reactions around a double C=C bond occur via conical intersections between the excited- and ground-state potential energy surfaces. In most cases, other coordinates than just the twist angle around the C=C bond are involved in the reaction, minimizing large-amplitude motion and thus allowing isomerization to take place in constrained environments.

DISCLOSURE STATEMENT

The authors are not aware of any affiliations, memberships, funding, or financial holdings that might be perceived as affecting the objectivity of this review.

ACKNOWLEDGMENTS

The authors would like to thank the University of Geneva, the Swiss National Science Foundation, and the NCCR MUST for financial support.

LITERATURE CITED

1. Shank CV. 1986. Investigation of ultrafast phenomena in the femtosecond time domain. *Science* 233:1276–80
2. Zinth W, Kaiser W. 1988. Ultrafast coherent spectroscopy. *Top. Appl. Phys.* 60:235–77
3. Khundkar LR, Zewail AH. 1990. Ultrafast molecular reaction dynamics in real-time: progress over a decade. *Annu. Rev. Phys. Chem.* 41:15–60

4. Suppan P. 1994. *Chemistry and Light*. Cambridge, UK: Cambridge Univ. Press
5. Chudoba C, Riedle E, Pfeiffer M, Elsaesser T. 1996. Vibrational coherence in ultrafast excited state proton transfer. *Chem. Phys. Lett.* 263:622–28
6. Douhal A, Lahmani F, Zewail AH. 1996. Proton-transfer reaction dynamics. *Chem. Phys.* 207:477–98
7. Takeuchi S, Tahara T. 2005. Coherent nuclear wavepacket motions in ultrafast excited-state intramolecular proton transfer: sub-30-fs resolved pump-probe absorption spectroscopy of 10-hydroxybenzo[h]quinoline in solution. *J. Phys. Chem. A* 109:10199–207
8. Schriever C, Lochbrunner S, Ofial AR, Riedle E. 2011. The origin of ultrafast proton transfer: multidimensional wave packet motion versus tunneling. *Chem. Phys. Lett.* 503:61–65
9. Sension RJ, Repinec ST, Szarka AZ, Hochstrasser RA. 1993. Femtosecond laser studies of the *cis*-stilbene photoisomerization reactions. *J. Chem. Phys.* 98:6291–315
10. Kukura P, McCamant DW, Yoon S, Wandschneider DB, Mathies RA. 2005. Structural observation of the primary isomerization in vision with femtosecond-stimulated Raman. *Science* 310:1006–9
11. Levine BG, Martínez TJ. 2006. Isomerization through conical intersections. *Annu. Rev. Phys. Chem.* 58:613–34
12. Wynne K, Reid GD, Hochstrasser RM. 1996. Vibrational coherence in electron transfer: the tetracyanoethylene-pyrene complex. *J. Chem. Phys.* 105:2287–98
13. Pagès S, Lang B, Vauthey E. 2004. Ultrafast spectroscopic investigation of the charge recombination dynamics of ion pairs formed upon highly exergonic bimolecular electron transfer quenching: looking for the normal region. *J. Phys. Chem. A* 108:549–55
14. **Horng ML, Gardecki JA, Papazyan A, Maroncelli M. 1995. Subpicosecond measurements of polar solvation dynamics: coumarin 153 revisited. *J. Phys. Chem.* 99:17311–37**
15. Kovalenko SA, Schanz R, Hennig H, Ernsting NP. 2001. Cooling dynamics of an optically excited molecular probe in solution from femtosecond broadband transient absorption spectroscopy. *J. Chem. Phys.* 115:3256–73
16. Pigliucci A, Duvanel G, Daku LML, Vauthey E. 2007. Investigation of the influence of solute-solvent interactions on the vibrational energy relaxation dynamics of large molecules in liquids. *J. Phys. Chem. A* 111:6135–45
17. Angulo G, Kattnig DR, Rosspeintner A, Grampp G, Vauthey E. 2010. On the coherent description of diffusion-influenced fluorescence quenching experiments II: early events. *Chem. Eur. J.* 16:2291–99
18. **Fragnito HL, Bigot JY, Becker PC, Shank CV. 1989. Evolution of the vibronic absorption spectrum in a molecule following impulsive excitation with a 6 fs optical pulse. *Chem. Phys. Lett.* 160:101–4**
19. Rubtsov IV, Yoshihara K. 1997. Oscillatory fluorescence decay of an electron donor-acceptor complex. *J. Phys. Chem. A* 101:6138–40
20. Kobayashi T, Saito T, Ohtani H. 2001. Real-time spectroscopy of transition states in bacteriorhodopsin during retinal isomerization. *Nature* 414:531–34
21. Teller E. 1937. The crossing of potential surfaces. *J. Phys. Chem.* 41:109–16
22. Michl J. 1974. Physical basis of qualitative MO arguments in organic photochemistry. *Top. Curr. Chem.* 46:1–59
23. Domcke W, Yarkony D, Köppel H, eds. 2004. *Conical Intersections: Electronic Structure, Dynamics and Spectroscopy*. Singapore: World Sci.
24. Dobryakov AL, Kovalenko SA, Weigel A, Perez-Lustres JL, Lange J, et al. 2010. Femtosecond pump/supercontinuum-probe spectroscopy: optimized setup and signal analysis for single-shot spectral referencing. *Rev. Sci. Instrum.* 81:113106
25. Zhang XX, Würth C, Zhao L, Resch-Genger U, Ernsting NP, Sajadi M. 2011. Femtosecond broadband fluorescence upconversion spectroscopy: improved setup and photometric correction. *Rev. Sci. Instrum.* 82:063108
26. Joo T, Jia Y, Yu J-Y, Jonas DM, Fleming GR. 1996. Dynamics in isolated bacterial light harvesting antenna (LH2) of *Rhodobacter sphaeroides* at room temperature. *J. Phys. Chem.* 100:2399–409
27. de Boeij WP, Pshenichnikov MS, Wiersma DA. 1998. Heterodyne-detected stimulated photon echo: applications to optical dynamics in solution. *Chem. Phys.* 233:287–309

14. Comprehensive experimental study on polar solvation dynamics serving as reference for average solvation times in many polar solvents.

18. First observation of vibrational wavepacket upon vibronic excitation of a dye in solution.

28. Brixner T, Stenger J, Waswani HM, Cho M, Blankenship RE, Fleming GR. 2005. Two dimensional electronic spectroscopy of electronic couplings in photosynthesis. *Nature* 434:625–28
29. Hamm P, Zanni M. 2011. *Concepts and Methods of 2D Infrared Spectroscopy*. Cambridge, UK: Cambridge Univ. Press
30. Fischer SF, Laubereau A. 1975. Dephasing processes of molecular vibrations in liquids. *Chem. Phys. Lett.* 35:6–12
31. Elsaesser T, Kaiser W. 1991. Vibrational and vibronic relaxation of large polyatomic molecules in liquids. *Annu. Rev. Phys. Chem.* 42:83–107
32. Hamm P, Ohline SM, Zinth W. 1997. Vibrational cooling after ultrafast photoisomerisation of azobene measured by femtosecond infrared spectroscopy. *J. Chem. Phys.* 106:519–30
33. Adamczyk K, Banerji N, Villamaina D, Dreyer J, Lang B, et al. 2011. Tracking the pathway of an ultrafast bimolecular electron transfer reaction. In *Ultrafast Phenomena XVII*, ed. M Chergui, D Jonas, E Riedle, R Schoenlein, A Taylor, pp. 376–78. New York: Oxford Univ. Press
34. Stephens MD, Saven JG, Skinner JL. 1997. Molecular theory of electronic spectroscopy in nonpolar fluids: ultrafast solvation dynamics and absorption and emission line shapes. *J. Chem. Phys.* 106:2129–44
35. Kubo R. 1957. Statistical-mechanical theory of irreversible processes. I. General theory and simple applications to magnetic and conduction problems. *J. Phys. Soc. Jpn.* 12:570–86

36. Modeling nonpolar solvation dynamics with a viscoelastic continuum model reveals a complex relationship between time-domain optical response and underlying molecular modes.

36. Berg M. 1998. Viscoelastic continuum model of nonpolar solvation. 1. Implications for multiple time scales in liquid dynamics. *J. Phys. Chem. A* 102:17–30
37. Berg MA, Rector KD, Fayer MD. 2000. Two-pulse echo experiments in the spectral diffusion regime. *J. Chem. Phys.* 113:3233–42
38. Biswas R, Bhattacharyya S, Bagchi B. 1998. Vibrational energy relaxation, nonpolar solvation dynamics and instantaneous normal modes: role of binary interaction in the ultrafast response of a dense liquid. *J. Chem. Phys.* 108:4963–71
39. Everitt KF, Skinner JL. 2001. Molecular theory of three-pulse photon echoes for solutes in non-polar fluids. *Chem. Phys.* 266:197–204
40. Larsen DS, Ohta K, Fleming GR. 1999. Three pulse photon echo studies of nondipolar solvation: comparison with a viscoelastic model. *J. Chem. Phys.* 111:8970–79

41. A continuum model for polar solvation and dielectric friction is worked out.

41. van der Zwan G, Hynes JT. 1985. Time-dependent fluorescence solvent shifts, dielectric friction, and nonequilibrium solvation in polar solvents. *J. Phys. Chem.* 89:4181–88
42. Giraud G, Wynne K. 2003. A comparison of the low-frequency vibrational spectra of liquids obtained through infrared and Raman spectroscopies. *J. Chem. Phys.* 119:11753–64
43. de Boeij WP, Pshenichnikov MS, Wiersma DA. 1996. On the relation between the echo-peak shift and Brownian-oscillator correlation function. *Chem. Phys. Lett.* 253:53–60
44. Fleming GR, Cho M. 1996. Chromophore-solvent dynamics. *Annu. Rev. Phys. Chem.* 47:109–34
45. Maroncelli M, Zhang X-X, Liang M, Roy D, Ernsting NP. 2011. Measurements of the complete solvation response of coumarin 153 in ionic liquids and the accuracy of simple dielectric continuum predictions. *Faraday Discuss.* 154:409–24
46. Turton DA, Wynne K. 2009. Universal nonexponential relaxation: complex dynamics in simple liquids. *J. Chem. Phys.* 131:201101
47. Bosma WB, Yan YJ, Mukamel S. 1990. Impulsive pump-probe and photon-echo spectroscopies of dye molecules in condensed phases. *Phys. Rev. A* 42:6920–23
48. Mukamel S. 1995. *Principles of Nonlinear Optical Spectroscopy*. New York: Oxford Univ. Press
49. Book LD, Scherer NF. 1999. Wavelength-resolved stimulated photon echoes: direct observation of ultrafast intramolecular vibrational contributions to electronic dephasing. *J. Chem. Phys.* 111:792–95
50. Lazonder K, Pshenichnikov MS. 2007. Solvent dynamics in a glass-forming liquid from 300 K to 3 K: what photon echoes can teach us. *Chem. Phys.* 341:123–42
51. Kennis JTM, Larsen DS, Ohta K, Facciotti MT, Glaeser RM, Fleming GR. 2002. Ultrafast protein dynamics of bacteriorhodopsin probed by photon echo and transient absorption spectroscopy. *J. Phys. Chem. B* 106:6067–80
52. Shirota H, Funston AM, Wishart JF, Castner EW. 2005. Ultrafast dynamics of pyrrolidinium cation ionic liquids. *J. Chem. Phys.* 122:184512

53. Prigogine I, Rice SA, eds. 1999. *Electron Transfer: From Isolated Molecules to Biomolecules.* Adv. Chem. Phys. 106 & 107. New York: Wiley
54. Balzani V, ed. 2001. *Electron Transfer in Chemistry*. New York: Wiley
55. Baranoff E, Barigelletti F, Bonnet S, Collin J-P, Flamigni L, et al. 2007. From photoinduced charge separation to light-driven molecular machines. *Struct. Bond.* 123:41–78
56. Prasanna de Silva A, Uchiyama S. 2011. Molecular logic gates and luminescent sensors based on photoinduced electron transfer. *Top. Curr. Chem.* 300:1–28
57. Gust D, Moore TA, Moore AL. 2009. Solar fuels via artificial photosynthesis. *Acc. Chem. Res.* 42:1890–98
58. Clarke TM, Durrant JR. 2010. Charge photogeneration in organic solar cells. *Chem. Rev.* 110:6736–67
59. Vauthey E. 2012. Photoinduced symmetry-breaking charge separation. *ChemPhysChem* 13:2001–11
60. Mataga N, Chosrowjan H, Taniguchi S. 2005. Ultrafast charge transfer in excited electronic states and investigations into fundamental problems of exciplex chemistry: our early studies and recent developments. *J. Photochem. Photobiol. C* 6:37–79
61. Vauthey E. 2006. Investigations of bimolecular photoinduced electron transfer reactions in polar solvents using ultrafast spectroscopy. *J. Photochem. Photobiol. A* 179:1–12
62. Marcus RA, Sutin N. 1985. Electron transfer in chemistry and biology. *Biochim. Biophys. Acta* 811:265–322
63. Jortner J, Ulstrup J. 1975. The effect of intramolecular quantum modes on free energy relationships for electron transfer reactions. *J. Chem. Phys.* 63:4358–68
64. Mataga N, Asahi T, Kanda Y, Okada T. 1988. The bell-shaped energy gap dependence of the charge recombination reaction of geminate radical ion pairs produced by fluorescence quenching reaction in acetonitrile solution. *Chem. Phys.* 127:249–61
65. Vauthey E. 2001. Direct measurements of the charge recombination dynamics of geminate ion pairs formed upon electron transfer quenching at high donor concentration. *J. Phys. Chem. A* 105:340–48
66. Wasielewski MR, Niemczyk NP, Svec WA, Pewitt EB. 1985. Dependence of rate constants for the photoinduced charge separation and dark charge recombination on free energy of reaction in restricted distance porphyrin quinone molecules. *J. Am. Chem. Soc.* 107:1080–82
67. Miller JR, Calcaterra LT, Closs GL. 1984. Intramolecular long distance electron transfer in radical anions: the effect of free energy and solvent on the reaction rates. *J. Am. Chem. Soc.* 106:3047–49
68. Mataga N, Chosrowjan H, Shibata Y, Yoshida N, Osuka A, et al. 2001. First unequivocal observation of the whole bell-shaped energy gap law in intramolecular charge separation from S_2 excited state of directly linked porphyrin-imide dyads and its solvent-polarity dependencies. *J. Am. Chem. Soc.* 123:12422–23
69. Rehm D, Weller A. 1970. Kinetic of fluorescence quenching by electron and hydrogen atom transfer. *Isr. J. Chem.* 8:259–71
70. Rosspeintner A, Kattnig DR, Angulo G, Landgraf S, Grampp G. 2008. The Rehm-Weller experiment in view of distant electron transfer. *Chem. Eur. J.* 14:6213–21
71. Burshtein AI, Ivanov AI. 2007. A diffusional alternative to the Marcus free energy gap law. *Phys. Chem. Chem. Phys.* 9:396–400
72. Masad A, Huppert D, Kosower EM. 1990. The transition from non-adiabatic to solvent controlled adiabatic electron transfer kinetics. *Chem. Phys.* 144:391–400
73. Barbara PF, Jarzeba W. 1990. Ultrafast photochemical intramolecular charge and excited state solvation. *Adv. Photochem.* 15:1–68
74. Schmidhammer U, Megerle U, Lochbrunner S, Riedle E, Karpiuk J. 2008. The key role of solvation dynamics in intramolecular electron transfer: time-resolved photophysics of crystal violet lactone. *J. Phys. Chem. A* 112:8487–96
75. Banerji N, Angulo G, Barabanov II, Vauthey E. 2008. Intramolecular charge-transfer dynamics in covalently linked perylene-dimethylaniline and cyanoperylene-dimethylaniline. *J. Phys. Chem. A* 112:9665–74
76. Rips I, Jortner J. 1987. Dynamic solvent effects on outer-sphere electron transfer. *J. Chem. Phys.* 87:2090–104
77. Heitele H. 1993. Dynamic solvent effects on electron transfer reactions. *Angew. Chem. Int. Ed. Engl.* 32:359–77
78. Kandori H, Kemnitz K, Yoshihara K. 1992. Subpicosecond transient absorption study of intermolecular electron transfer between solute and electron-donating solvents. *J. Phys. Chem.* 96:8042–48

77. Comprehensive overview of the effect of solvent dynamics on electron transfer reactions.

79. Xu Q-H, Scholes GD, Yang M, Fleming GR. 1999. Probing solvation and reaction coordinates of ultrafast photoinduced electron-transfer reactions using nonlinear spectroscopies: rhodamine 6G in electron-donating solvents. *J. Phys. Chem. A* 103:10348–58
80. Smith NA, Lin S, Meech SR, Shirota H, Yoshihara K. 1997. Ultrafast dynamics of liquid anilines studied by the optical Kerr effect. *J. Phys. Chem. A* 101:9578–86
81. Sumi H, Marcus RA. 1986. Dynamical effects in electron transfer reactions. *J. Chem. Phys.* 84:4894–14
82. Walker GC, Akesson E, Johnson AE, Levinger NE, Barbara PF. 1992. Interplay of solvent motion and vibrational excitation in electron transfer kinetics: experiment and theory. *J. Phys. Chem.* 96:3728–36
83. Nicolet O, Vauthey E. 2002. Ultrafast nonequilibrium charge recombination dynamics of excited donor-acceptor complexes. *J. Phys. Chem. A* 106:5553–62

84. The ultrafast charge recombination dynamics of excited donor-acceptor complex is shown to depend on the excitation wavelength.

84. Nicolet O, Banerji N, Pagès S, Vauthey E. 2005. Effect of the excitation wavelength on the ultrafast charge recombination dynamics of donor-acceptor complexes in polar solvents. *J. Phys. Chem. A* 109:8236–45
85. Mohammed OF, Vauthey E. 2008. Simultaneous generation of different types of ion pairs upon charge-transfer excitation of a donor-acceptor complex revealed by ultrafast transient absorption spectroscopy. *J. Phys. Chem. A* 112:5804–9
86. Feskov SV, Ionkin VN, Ivanov AI. 2006. Effect of high-frequency modes and hot transitions on free energy gap dependence of charge recombination rate. *J. Phys. Chem. A* 110:11919–25
87. Ivanov AI, Belikeev FN, Fedunov RG, Vauthey E. 2003. The effect of excitation pulse carrier frequency on ultrafast charge recombination dynamics of excited donor-acceptor complexes. *Chem. Phys. Lett.* 372:73–81
88. Fedunov RG, Ivanov AI. 2005. Effect of the excitation pulse frequency on the ultrafast photoinduced electron transfer dynamics. *J. Chem. Phys.* 122:064501
89. Fedunov RG, Feskov SV, Ivanov AI, Nicolet O, Pagès S, Vauthey E. 2004. Effect of the excitation pulse carrier frequency on the ultrafast charge recombination dynamics of donor-acceptor complexes: stochastic simulations and experiments. *J. Chem. Phys.* 121:3643–56
90. Gladkikh VS, Burshtein AI, Feskov SV, Ivanov AI, Vauthey E. 2005. Hot recombination of photogenerated ion pairs. *J. Chem. Phys.* 123:244510
91. Dilthey S, Stock G. 2002. Periodic-orbit analysis of coherent electron-transfer femtosecond experiments. *J. Phys. Chem. A* 106:8483–87
92. Pisliakov AV, Gelin MF, Domcke W. 2003. Detection of electronic and vibrational coherence effects in electron-transfer systems by femtosecond time-resolved fluorescence spectroscopy: theoretical aspects. *J. Phys. Chem. A* 107:2657–66
93. Rubtsov IV, Yoshihara K. 1999. Vibrational coherence in electron donor-acceptor complexes. *J. Phys. Chem. A* 103:12202–12
94. Seel M, Engleitner S, Zinth W. 1997. Wavepacket motion and ultrafast electron transfer in the system oxazine 1 in *N*,*N*-dimethylaniline. *Chem. Phys. Lett.* 275:363–69
95. Wolfseder B, Seidner L, Domcke W, Stock G, Seel M, et al. 1998. Vibrational coherence in ultrafast electron transfer dynamics of oxazine 1 in *N*,*N*-dimethylaniline: simulation of a femtosecond pump-probe experiment. *Chem. Phys.* 233:323–34
96. Engleitner S, Seel M, Zinth W. 1999. Nonexponentialities in the ultrafast electron-transfer dynamics in the system oxazine 1 in *N*,*N*-dimethylaniline. *J. Phys. Chem. A* 103:3013–19
97. Marcus RA. 1968. Theoretical relations among rate constants, barriers, and Broensted slopes of chemical reactions. *J. Phys. Chem.* 72:891–99
98. Agmon N, Levine RD. 1977. Energy, entropy and the reaction coordinate: thermodynamic-like relations in chemical kinetics. *Chem. Phys. Lett.* 52:197–201
99. Kiefer PM, Hynes JT. 2010. Theoretical aspects of tunneling proton transfer reactions in a polar environment. *J. Phys. Org. Chem.* 23:632–46
100. Kiefer PM, Hynes JT. 2004. Adiabatic and nonadiabatic proton transfer rate constants in solution. *Solid State Ion.* 168:219–24
101. Borgis D, Hynes JT. 1996. Curve crossing formulation for proton transfer reactions in solution. *J. Phys. Chem.* 100:1118–28

102. Peters KS, Cashin A, Timbers P. 1999. Picosecond dynamics of nonadiabatic proton transfer: a kinetic study of proton transfer within the contact radical ion pair of substituted benzophenones/*N*,*N*-dimethylaniline. *J. Am. Chem. Soc.* 122:107–13
103. Andrieux CP, Gamby J, Hapiot P, Savéant J-M. 2003. Evidence for inverted region behavior in proton transfer to carbanions. *J. Am. Chem. Soc.* 125:10119–24
104. Edwards SJ, Soudackov AV, Hammes-Schiffer S. 2009. Driving force dependence of rates for nonadiabatic proton and proton-coupled electron transfer: conditions for inverted region behavior. *J. Phys. Chem. B* 113:14545–48
105. Masuda Y, Nakano T, Sugiyama M. 2012. First observation of ultrafast intramolecular proton transfer rate between electronic ground states in solution. *J. Phys. Chem. A* 116:4485–94
106. Formosinho SJ, Arnaut LG. 1993. Excited-state proton transfer reactions II. Intramolecular reactions. *J. Photochem. Photobiol. A* 75:21–48
107. Waluk J. 2000. Conformational aspects of intra- and intermolecular excited-state proton transfer. In *Conformational Analysis of Molecules in Excited States*, ed. AP Marchand, pp. 57–112. New York: Wiley
108. Elsaesser T, Bakker HJ, eds. 2002. *Ultrafast Hydrogen Bonding Dynamics and Proton Transfer Processes in the Condensed Phase*. New York: Kluwer Acad.
109. Ädelroth P. 2006. Special issue on proton transfer in biological systems. *Biochim. Biophys. Acta* 1757:867–70
110. Meech SR. 2009. Excited state reactions in fluorescent proteins. *Chem. Soc. Rev.* 38:2922–34
111. Agmon N. 2004. Elementary steps in excited-state proton transfer. *J. Phys. Chem. A* 109:13–35
112. Tolbert LM, Solntsev KM. 2002. Excited-state proton transfer: from constrained systems to "super" photoacids to superfast proton transfer. *Acc. Chem. Res.* 35:19–27
113. Gutman M, Huppert D. 1979. Rapid pH and $\Delta\mu H^+$ jump by short laser pulse. *J. Biochem. Biophys. Methods* 1:9–19
114. Mohammed OF, Pines D, Dreyer J, Pines E, Nibbering ETJ. 2005. Sequential proton transfer through water bridges in acid-base reactions. *Science* 310:83–86
115. Adamczyk K, Prémont-Schwarz M, Pines D, Pines E, Nibbering ETJ. 2009. Real-time observation of carbonic acid formation in aqueous solution. *Science* 326:1690–94
116. Nosenko Y, Wiosna-Sałyga G, Kunitski M, Petkova I, Singh A, et al. 2008. Proton transfer with a twist? Femtosecond dynamics of 7-(2-pyridyl)indole in condensed phase and in supersonic jets. *Angew. Chem. Int. Ed. Engl.* 47:6037–40
117. Takeuchi S, Tahara T. 2007. The answer to concerted versus step-wise controversy for the double proton transfer mechanism of 7-azaindole dimer in solution. *Proc. Natl. Acad. Sci. USA* 104:5285–90
118. Kwon O-H, Zewail AH. 2007. Double proton transfer dynamics of model DNA base pairs in the condensed phase. *Proc. Natl. Acad. Sci. USA* 104:8703–8
119. Weinberg DR, Gagliardi CJ, Hull JF, Murphy CF, Kent CA, et al. 2012. Proton-coupled electron transfer. *Chem. Rev.* 112:4016–93
120. Cukier RI, Nocera DG. 1998. Proton-coupled electron transfer. *Annu. Rev. Phys. Chem.* 49:337–69
121. Shemesh D, Sobolewski AL, Domcke W. 2009. Efficient excited-state deactivation of the Gly-Phe-Ala tripeptide via an electron-driven proton-transfer process. *J. Am. Chem. Soc.* 131:1374–75
122. Hammes-Schiffer S, Stuchebrukhov AA. 2010. Theory of coupled electron and proton transfer reactions. *Chem. Rev.* 110:6939–60
123. Rosenthal J, Nocera DG. 2007. Role of proton-coupled electron transfer in O-O bond activation. *Acc. Chem. Res.* 40:543–53
124. Dempsey JL, Brunschwig BS, Winkler JR, Gray HB. 2009. Hydrogen evolution catalyzed by cobaloximes. *Acc. Chem. Res.* 42:1995–2004
125. Stubbe J, Nocera DG, Yee CS, Chang MCY. 2003. Radical initiation in the class I ribonucleotide reductase: long-range proton-coupled electron transfer? *Chem. Rev.* 103:2167–202
126. Kumar A, Sevilla MD. 2010. Proton-coupled electron transfer in DNA on formation of radiation-produced ion radicals. *Chem. Rev.* 110:7002–23
127. Prezhdo OV, Duncan WR, Prezhdo VV. 2008. Dynamics of the photoexcited electron at the chromophore-semiconductor interface. *Acc. Chem. Res.* 41:339–48

128. Hammes-Schiffer S. 2012. Proton-coupled electron transfer: classification scheme and guide to theoretical methods. *Energy Environ. Sci.* 5:7696–703
129. Navrotskaya I, Hammes-Schiffer S. 2009. Electrochemical proton-coupled electron transfer: beyond the golden rule. *J. Chem. Phys.* 131:024112
130. Hammes-Schiffer S. 2011. Current theoretical challenges in proton-coupled electron transfer: electron-proton nonadiabaticity, proton relays, and ultrafast dynamics. *J. Phys. Chem. Lett.* 2:1410–16
131. Soudackov AV, Hazra A, Hammes-Schiffer S. 2011. Multidimensional treatment of stochastic solvent dynamics in photoinduced proton-coupled electron transfer processes: sequential, concerted, and complex branching mechanisms. *J. Chem. Phys.* 135:144115
132. Irebo T, Reece SY, Sjödin M, Nocera DG, Hammarström L. 2007. Proton-coupled electron transfer of tyrosine oxidation: buffer dependence and parallel mechanisms. *J. Am. Chem. Soc.* 129:15462–64
133. van Thor JJ. 2009. Photoreactions and dynamics of the green fluorescent protein. *Chem. Soc. Rev.* 38:2935–50
134. Kimura Y, Fukuda M, Suda K, Terazima M. 2010. Excited state intramolecular proton transfer reaction of 4'-*N*,*N*-diethylamino-3-hydroxyflavone and solvation dynamics in room temperature ionic liquids studied by optical Kerr gate fluorescence measurement. *J. Phys. Chem. B* 114:11847–58
135. Hsieh C-C, Jiang C-M, Chou P-T. 2010. Recent experimental advances on excited-state intramolecular proton coupled electron transfer reaction. *Acc. Chem. Res.* 43:1364–74
136. Ameer-Beg S, Ormson SM, Brown RG, Matousek P, Towrie M, et al. 2001. Ultrafast measurements of excited state intramolecular proton transfer (ESIPT) in room temperature solutions of 3-hydroxyflavone and derivatives. *J. Phys. Chem. A* 105:3709–18

137. The first step in vision is shown to take place within 200 fs.

137. Schoenlein RW, Peteanu LA, Mathies RA, Shank CV. 1991. The first step in vision: femtosecond isomerisation of rhodopsin. *Science* 254:412–15

138. Polli D, Altoe P, Weingart O, Spillane KM, Manzoni C, et al. 2010. Conical intersection dynamics of the primary photoisomerization event in vision. *Nature* 467:440–43
139. Orlandi G, Siebrand W. 1975. Model for the direct photo-isomerization of stilbene. *Chem. Phys. Lett.* 30:352–54
140. Akesson E, Sundström V, Gillbro T. 1985. Solvent dependent barrier heights of excited state photoisomerisation reactions. *Chem. Phys. Lett.* 121:513–22
141. Xu QH, Fleming GR. 2001. Isomerisation dynamics of 1,1′-diethyl-4,4′-cyanine (1144C) studied by different third-order nonlinear spectroscopic measurements. *J. Phys. Chem. A* 105:10187–95
142. Mathies RA, Cruz CH, Pollard WT, Shank CV. 1988. Direct observation of the femtosecond excited state *cis-trans* isomerisation in bacteriorhodopsin. *Science* 240:777–79
143. Lochbrunner S, Fuss W, Schmid WE, Kompa K-L. 1998. Electronic relaxation and ground-state dynamics of 1,3-cyclohexadiene and *cis*-hexatriene in ethanol. *J. Phys. Chem. A* 102:9334–44
144. Bonačić-Koutecký V, Köhler J, Michl J. 1984. Prediction of structural and environmental effects on the S_1-S_0 energy gap and jump probability in double-bond *cis-trans* photoisomerization: a general rule. *Chem. Phys. Lett.* 104:440–43
145. Garavelli M, Celani P, Yamamoto N, Bernardi F, Robb MA, Olivucci M. 1996. The structure of the nonadiabatic photochemical *trans-cis* isomerization channel in all-*trans* octatetraene. *J. Am. Chem. Soc.* 118:11656–57
146. Quenneville J, Martínez TJ. 2003. Ab initio study of *cis-trans* photoisomerization in stilbene and ethylene. *J. Phys. Chem. A* 107:829–37
147. Kramers HA. 1940. Brownian motion in a field of force and the diffusion model of chemical reactions. *Physica* 7:284–304
148. Fleming GR. 1986. *Chemical Applications of Ultrafast Spectroscopy*. New York: Oxford Univ. Press
149. Velsko SP, Waldeck DH, Fleming GR. 1983. Breakdown of Kramers theory description of photochemical isomerisation and the possible involvement of frequency dependent friction. *J. Chem. Phys.* 78:249–58
150. Anderton RM, Kauffman JF. 1995. Isodielectric Kramers-Hubbard analysis of diphenylbutadiene photoisomerisation in alkylnitriles and chlorinated solvents. *J. Phys. Chem.* 99:14628–31
151. Sun YP, Saltiel J. 1989. Application of the Kramers equation to stilbene photoisomerisation in *n*-alkanes using translational diffusion coefficients to define microviscosity. *J. Phys. Chem.* 93:8310–16

152. Grote HF, Hynes JT. 1980. The stable states picture of chemical reactions. II. Rate constants for condensed and gas phase reaction models. *J. Chem. Phys.* 73:2715–32
153. Rothenberger G, Negus DK, Hochstrasser RM. 1983. Solvent influence on photoisomerisation dynamics. *J. Chem. Phys.* 79:5360–67
154. Sivakumar N, Hoburg EA, Waldeck DH. 1989. Solvent dielectric effects on isomerisation dynamics: investigation of the photoisomerisation of 4,4′-dimethoxystilbene and *t*-stilbene in *n*-alkyl nitriles. *J. Chem. Phys.* 90:2305–16
155. Vauthey E. 1995. Isomerisation dynamics of a thiacarbocyanine dye in different electronic states and in different classes of solvents. *Chem. Phys.* 196:569–82
156. Liu RS, Asato AE. 1985. The primary process of vision and the structure of bathorhodopsin: a mechanism for photoisomerization of polyenes. *Proc. Natl. Acad. Sci. USA* 82:259–63
157. Müller AM, Lochbrunner S, Schmid WE, Fuss W. 1998. Low-temperature photochemistry of previtamin D: a hula-twist isomerization of a triene. *Angew. Chem. Int. Ed. Engl.* 37:505–7
158. Imamoto Y, Kuroda T, Kataoka M, Shevyakov S, Krishnamoorthy G, Liu RS. 2003. Photoisomerization by hula twist: 2,2′-dimethylstilbene and a ring-fused analogue. *Angew. Chem. Int. Ed. Engl.* 42:3630–33
159. Litvinenko KL, Webber NM, Meech SR. 2003. Internal conversion in the chromophore of the green fluorescent protein: temperature dependence and isoviscosity analysis. *J. Phys. Chem. A* 107:2616–23
160. Vengris M, van Stokkum IHM, He X, Bell AF, Tonge PJ, et al. 2004. Ultrafast excited and ground-state dynamics of the green fluorescent protein chromophore in solution. *J. Phys. Chem. A* 108:4587–98
161. Wachtveitl J, Zumbusch A. 2011. Azobenzene: an optical switch for in vivo experiments. *ChemBioChem* 12:1169–70
162. Muraoka T, Kinbara K, Aida T. 2006. Mechanical twisting of a guest by a photoresponsive host. *Nature* 440:512–15
163. Kim M, Safron NS, Huang C, Arnold MS, Gopalan P. 2011. Light-driven reversible modulation of doping in graphene. *Nano Lett.* 12:182–87
164. Rau H, Lueddecke E. 1982. On the rotation-inversion controversy on photoisomerization of azobenzenes: experimental proof of inversion. *J. Am. Chem. Soc.* 104:1616–20
165. Nägele T, Hoche R, Zinth W, Wachtveitl J. 1997. Femtosecond photoisomerization of *cis*-azobenzene. *Chem. Phys. Lett.* 272:489–95
166. Fujino T, Arzhantsev SY, Tahara T. 2002. Femtosecond/picosecond time-resolved spectroscopy of *trans*-azobenzene: isomerization mechanism following $S_2(\pi\pi^*) \leftarrow S_0$ photoexcitation. *Bull. Chem. Soc. Jpn.* 75:1031–40
167. Schultz T, Quenneville J, Levine B, Toniolo A, Martínez TJ, et al. 2003. Mechanism and dynamics of azobenzene photoisomerization. *J. Am. Chem. Soc.* 125:8098–99
168. Hoffman DP, Mathies RA. 2012. Photoexcited structural dynamics of an azobenzene analog 4-nitro-4′-dimethylamino-azobenzene from femtosecond stimulated Raman. *Phys. Chem. Chem. Phys.* 14:6298–306
169. von Smoluchowski M. 1918. Versuch einer mathematischen Theorie der Koagulationskinetik kolloider Lösungen. *Z. Phys. Chem.* 92:129–68
170. Collins FC, Kimball GE. 1949. Diffusion-controlled reaction rates. *J. Colloid Sci.* 4:425–37
171. Burshtein AI. 2004. Non-Markovian theories of transfer reactions in luminescence and chemiluminescence and photo- and electrochemistry. In *Advances in Chemical Physics*, ed. SA Rice, 129:105–418. Hoboken, NJ: Wiley
172. Murata S, Matsuzaki SY, Tachiya M. 1995. Transient effect in fluorescence quenching by electron transfer. 2. Determination of the rate parameters involved in the Marcus equation. *J. Phys. Chem.* 99:5354–58
173. Weidemaier K, Tavernier HL, Swallen SF, Fayer MD. 1997. Photoinduced electron transfer and geminate recombination in liquids. *J. Phys. Chem. A* 101:1887–902
174. Cohen B, Huppert D, Agmon N. 2000. Non-exponential Smoluchowski dynamics in fast acid-base reaction. *J. Am. Chem. Soc.* 122:9838–39
175. Solntsev K, Huppert D, Agmon N. 2001. Experimental evidence for a kinetic transition in reversible reactions. *Phys. Rev. Lett.* 86:3427–30

156. The hula-twist mechanism is proposed to account for ultrafast *cis-trans* isomerization in a constrained environment.

169. First theoretical description of a time-dependent rate coefficient.

Annual Review of
Physical Chemistry
Volume 64, 2013

Contents

Indexes

Errata

An online log of corrections to *Annual Review of Physical Chemistry* articles may be found at http://physchem.annualreviews.org/errata.shtml